

## Theory of two-dimensional oblique dispersive shock waves in supersonic flow of a superfluid

M. A. Hoefer<sup>1,\*</sup> and B. Ilan<sup>2</sup>

<sup>1</sup>*Department of Applied Physics and Applied Mathematics, Columbia University, New York, New York 10027, USA*

<sup>2</sup>*School of Natural Sciences, University of California, Merced, California 95343, USA*

(Received 2 June 2009; published 4 December 2009)

Dispersive shock waves (DSWs) are studied theoretically in the context of two-dimensional (2D) supersonic flow of a superfluid. Employing Whitham averaging theory for the repulsive Gross-Pitaevskii (GP) equation, suitable jump and entropy conditions are obtained for an oblique DSW, a fundamental building block for 2D flows with boundaries. In analogy to oblique viscous shock waves (VSWs), these conditions yield analytic relations between Mach number ( $M$ ), velocity deflection angle ( $\theta$ ), and wave angle ( $\beta$ ). Unlike VSWs, the  $M$ - $\theta$ - $\beta$  phase diagram for DSWs displays four distinct regions associated with phase transitions in supersonic flow over a corner which are predicted and verified by numerical computations of the GP equation. Quasistationary DSWs, shock detachment due to transonic flow, spontaneous excitation of vortices, and the onset of turbulent dynamics associated with cavitation of the superfluid are observed.

DOI: [10.1103/PhysRevA.80.061601](https://doi.org/10.1103/PhysRevA.80.061601)

PACS number(s): 03.75.Kk, 47.40.Nm, 03.75.Lm, 42.65.Sf

One of the hallmarks of supersonic flows is the formation of shock waves, which are nonlinear disturbances in the fluid's material and thermodynamic properties. In dissipative media, self-steepening can lead to the formation of viscous shock waves (VSWs), which are localized, sharp jumps in the fluid properties. Geometry plays a key role in VSW formation: a two-dimensional (2D) supersonic flow when turned through a compression, e.g., by an obstacle, can lead to a VSW. Straight, oblique, and curved detached VSWs can form when the flow is supersonic or transonic, respectively [1]. These stationary shock patterns can exhibit stable rich dynamical behavior [2] and have recently found application in the study of granular flows [3].

On the other hand, dispersive shock waves (DSWs) are expanding, rapidly oscillating disturbances that connect two disparate regions in a nonlinear dispersive medium, such as a superfluid flowing at supersonic speed. The study of DSWs dates back to shallow water systems (see, e.g., [4]) and have been observed in multiple branches of physics including astrophysical plasma [5], ultracold atoms [6,7], and nonlinear optics [8]. However, with few exceptions [9–13], the entire body of DSW theory literature has been confined to one dimension. In particular, the one-dimensional (1D) theory of Whitham averaging has been very successful but has proven difficult to generalize to higher dimensions perhaps due to complexities in the resulting modulation equations [14].

The different methods derived in this Rapid Communication open a different avenue for analyzing multidimensional DSWs. We show that the rudiments of 1D DSW theory, i.e., Whitham averaging, can be extended to multiple dimensions. This is achieved by constructing analytically what is arguably the simplest 2D dispersive shock structure, an oblique DSW, from which more complex structures can be “built.” Hence, this work addresses an outstanding problem in DSW theory that has arisen across multiple branches of physics. In addition, we numerically observe rich and complex 2D DSW

flows across corners, very different from the analogous 1D “piston problem” [15], and explain precisely how this richness arises from the multidimensional DSW theory. The broader message of this work is that multidimensional supersonic flows can be understood in terms of a unified approach that is based on simpler 1D “building blocks.”

We begin by constructing an oblique DSW for the repulsive Gross-Pitaevskii (GP) or defocusing nonlinear Schrödinger (NLS) equation. Relations between the upstream and downstream flow properties are derived resulting in the Mach number-deflection angle-DSW wave angle ( $M$ - $\theta$ - $\beta$ ) phase diagram. We study the case of flow over a corner where four distinct regimes in the phase diagram are related to numerical simulations of the (2+1)D GP equation. A suite of phase transitions depending on Mach number and corner angle are observed. Persistent quasistationary DSW patterns, shock detachment with spontaneous vortex pair creation, and turbulent dynamics are related directly to the  $M$ - $\theta$ - $\beta$  diagram prediction of fully supersonic flow, transonic flow, and cavitation of the superfluid, respectively. Such behavior does not exist in dissipative media and is experimentally accessible in condensed matter and optical systems, complementing recent studies of shock waves [6–8,16], phase transitions [17], and turbulence [18].

We consider systems governed by the 2D repulsive GP equation in the semiclassical (small dispersion) regime, which in nondimensional form is

$$i\varepsilon\psi_t = -\frac{\varepsilon^2}{2}\nabla^2\psi + V\psi + |\psi|^2\psi, \quad \nabla^2 = \frac{\partial^2}{\partial x^2} + \frac{\partial^2}{\partial y^2}, \quad (1)$$

where  $\psi(x, y, t)$  is a complex-valued field,  $V(x, y, t)$  is a linear potential that models a moving obstacle, and  $0 < \varepsilon \ll 1$  is a normalized dispersion coefficient. Equation (1) models a 2D BEC in the mean-field approximation [19] and also models the envelope of a light beam propagating through a defocusing nonlinear medium [20] which can be interpreted as an optical “superfluid” [21].

Equation (1) admits oblique dark soliton solutions which experience a transverse, “snake” instability that is of either

\*Present address: Department of Mathematics, North Carolina State University, Raleigh, NC 27695, USA; mahoefer@ncsu.edu

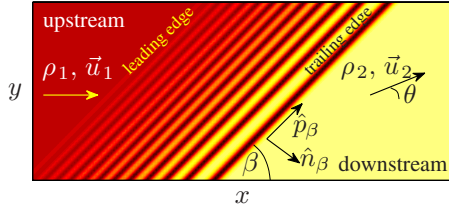


FIG. 1. (Color online) Density of an oblique DSW. Lighter regions correspond to larger density.

the absolute or convective type [13]. A convective instability practically means that the soliton is stable in a region close to the obstacle where growing perturbations (e.g., vortices) are “carried away” by the flow. Recent theoretical studies of supersonic flows past an obstacle found oblique soliton trains [10], oblique dark solitons [12], and the formation of small-amplitude “ship waves” [13].

We now consider the (2+1)D GP Eq. (1) with  $V \equiv 0$  to construct an oblique DSW. Employing the transformation  $\psi = \sqrt{\rho} \exp(i\phi/\varepsilon)$ , where  $\rho$  is the fluid density and  $\vec{u} = \nabla \phi$  is the velocity, leads to the Euler-like equations

$$\rho_t + \nabla \cdot (\rho \vec{u}) = 0,$$

$$(\rho \vec{u})_t + \nabla \cdot (\rho \vec{u} \otimes \vec{u}) + \frac{1}{2} \nabla \rho^2 = \frac{\varepsilon^2}{4} \rho \nabla \left[ \frac{\nabla^2 \rho}{\rho} - \frac{|\nabla \rho|^2}{2\rho^2} \right]. \quad (2)$$

When  $\varepsilon=0$ , Eqs. (2) reduce to the shallow water equations or the isentropic compressible gas equations [1]. When a steep gradient forms, the dispersive term becomes large and can lead to the formation of a DSW, which can be oblique, i.e., form an angle with the incoming flow direction (see Fig. 1).

We restrict the wave propagation direction to  $\pi/2 + \beta$  (see Fig. 1) and rotate the coordinates of Eqs. (2) as

$$\xi = \sin(\beta)x - \cos(\beta)y, \quad (3)$$

leading to a (1+1)D GP equation with  $\nabla \rightarrow \hat{\xi} \partial / \partial \xi$ . We now derive the relations between the up and downstream flows by considering the oblique Riemann initial data

$$\rho(x, y, 0) = \begin{cases} \rho_1 & \xi < 0 \\ \rho_2 & \xi > 0, \end{cases} \quad (4)$$

$$\vec{u}(x, y, 0) = \begin{cases} u_1 [1, 0] & \xi < 0 \\ u_2 [\cos(\theta), \sin(\theta)] & \xi > 0, \end{cases}$$

where  $\theta$  is the deflection angle; then we can use 1D DSW theory based on the Whitham averaging method for the (1+1) D NLS-GP equation [7,22,23].

To first order in  $\varepsilon$ , a normal DSW can be described by a slowly modulated elliptic function with a dark-soliton train at the trailing edge decaying to small amplitude linear waves at the leading edge. It can exist when suitable jump and entropy conditions are satisfied for a so-called simple wave across the shock front. We let  $\hat{n}_\beta = [\sin(\beta), -\cos(\beta)]$  and  $\hat{p}_\beta = [\cos(\beta), \sin(\beta)]$  be the unit vectors normal and parallel to the DSW trailing edge, respectively (Fig. 1). Assuming that

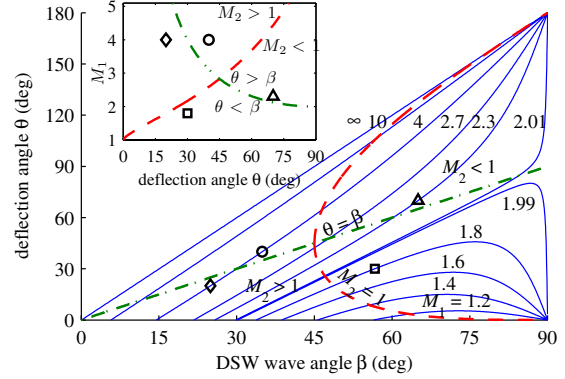


FIG. 2. (Color online)  $M$ - $\theta$ - $\beta$  phase diagram [relations (7) and (8)] showing the deflection angle  $\theta$  as a function of the wave angle  $\beta$  for various supersonic upstream Mach numbers  $M_1 > 1$ . Inset: Sonic Mach number  $M_s(\theta)$  (dashed curve) and cavitation sonic Mach number  $M_{cav}(\theta)$  (dash-dotted curve). Geometric symbols correspond to the simulation parameters in Fig. 3.

the parallel velocity is continuous across the shock and the normal velocity satisfies the simple wave conditions for a normal DSW [22] leads to the oblique DSW *jump conditions*

$$(\vec{u}_1 - \vec{u}_2) \cdot \hat{n}_\beta = 2(\sqrt{\rho_2} - \sqrt{\rho_1}), \quad (\vec{u}_1 - \vec{u}_2) \cdot \hat{p}_\beta = 0. \quad (5)$$

The jump conditions [Eq. (5)] are justified by the restricted flow direction [Eq. (3)] and the irrotationality of the flow,  $\partial u_x / \partial y - \partial u_y / \partial x = 0$ . We can simplify [Eq. (5)] in the reference frame moving with the soliton trailing edge [22]

$$v_{\text{trail}} = -\sqrt{\rho_2} + \vec{u}_1 \cdot \hat{n}_\beta = 0. \quad (6)$$

According to Eqs. (2) small amplitude disturbances propagate with the sound speed  $\sqrt{\rho}$ . We therefore introduce the local Mach numbers as  $M_i = u_i / \sqrt{\rho_i}$ ,  $i=1,2$ . Combining Eqs. (5) and (6), we obtain the following relations between the deflection angle  $\theta$  and DSW wave angle  $\beta$ :

$$\tan(\beta - \theta) = 2 \sec(\beta) / M_1 - \tan(\beta). \quad (7)$$

Relation (7) is depicted in Fig. 2. Much like a VSW, a DSW must also satisfy an *entropy condition*:  $\rho_2 > \rho_1$  [22]. This restricts its region of existence to

$$M_1 > 1, \quad 0 < \theta \leq \pi, \quad \sin^{-1}(1/M_1) < \beta \leq \pi/2. \quad (8)$$

Hence an oblique DSW requires a supersonic upstream flow, a positive deflection angle so that the flow always turns *into* the DSW, and a DSW wave angle larger than the so-called Mach angle  $\sin^{-1}(1/M_1)$ , the same as an oblique VSW [1].

Relations (7) and (8) accompanied by the  $M$ - $\theta$ - $\beta$  phase diagram in Fig. 2 are the main results of this Rapid Communication. They represent the fundamental conditions for the existence of an oblique DSW according to the (2+1)D NLS/GP Eq. (1) and provide insight into flows around obstacles, as discussed below. This  $M$ - $\theta$ - $\beta$  phase diagram is markedly different from that for an oblique VSW in gas dynamics [1] (chapter 4) and in shallow water flows (cf. [3]) when  $M_1 > 2$ . In the oblique VSW case it is impossible for  $\theta > \beta$  and it is always true that  $\theta < \pi/2$ .

When a supersonic flow encounters an obstacle, an “at-

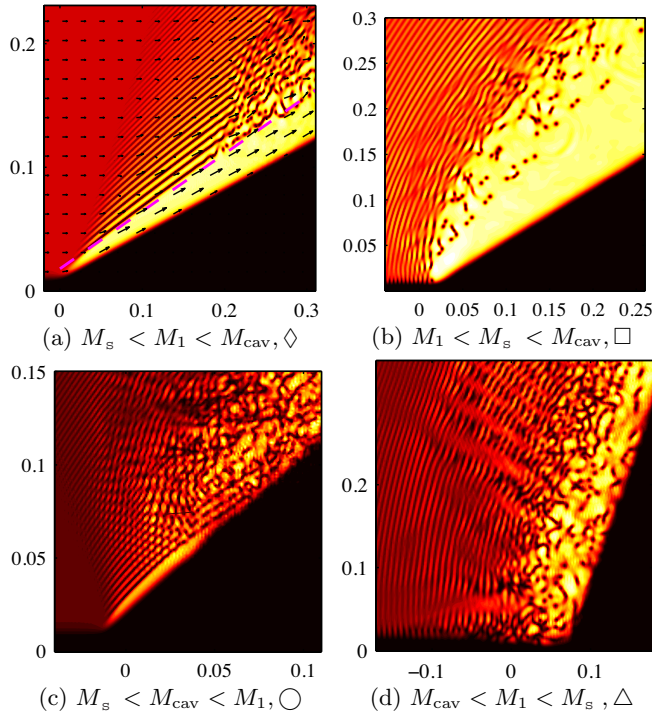


FIG. 3. (Color online) Density plots in the  $x$ - $y$  plane of flows past a corner with angle  $\theta$  and Mach number  $M_1$ . (a)  $\theta=20^\circ$ ,  $M_1=4$ ,  $t=0.12$  [momentum field depicted by arrows, dashed line is predicted by the DSW wave angle from Eq. (7)], (b)  $\theta=30^\circ$ ,  $M_1=1.8$ ,  $t=0.23$ , (c)  $\theta=40^\circ$ ,  $M_1=4$ ,  $t=0.086$ , and (d)  $\theta=70^\circ$ ,  $M_1=2.3$ ,  $t=0.15$ . See [25] for animations and a momentum plot identifying a vortex pair of opposite polarity.

tached” or “detached,” curved oblique shock wave can be excited if the downstream flow is supersonic or subsonic (the transonic regime [1]), respectively. This maxim holds true for DSWs also. Using Eqs. (5) and (6), the downstream Mach number is

$$M_2 = \cot(\beta)\sec(\beta - \theta). \quad (9)$$

Equation (9) for a sonic downstream flow,  $M_2=1$ , along with Eq. (7) determine a sonic wave angle  $\beta_s(M_1)$  and sonic deflection angle  $\theta_s(M_1)$  satisfying  $\sin(\beta_s) = -2/M_1 + \sqrt{1+8/M_1^2}$  and  $\cos(\theta_s) = (10\sqrt{8+M_1^2} - M_1^2 - 28)/(M_1\sqrt{12+M_1^2 - 4\sqrt{8+M_1^2}})$  (dashed curves in Fig. 2 and inset). Inverting the latter, we find that the *sonic upstream Mach number*,  $M_s(\theta)$ , divides the phase space  $(M_1, \theta)$  into supersonic ( $M_1 > M_s$ ) and transonic ( $M_1 < M_s$ ) regimes.

A behavior peculiar to an oblique DSW is that fluid can flow into it from both sides ( $\theta > \beta$ ), an impossibility for an oblique VSW. Using Eqs. (7) and (6), the transition to this behavior,  $\theta = \beta$ , occurs when  $\sqrt{\rho_2/\rho_1} = M_1 \sin(\theta) = 2$  or precisely when a vacuum line forms (cavitation) in the oblique DSW [24]. We define the *cavitation Mach number* when  $\theta = \beta$ ,  $M_{\text{cav}}(\theta) = 2/\sin(\theta)$  (dash-dotted curves in Fig. 2 and inset) so that cavitation occurs when  $M_1 > M_{\text{cav}}$ . Since  $M_{\text{cav}} \geq 2$ , only the isolated range  $1 < M_1 < 2$  gives rise to oblique DSWs comparable to oblique VSWs [1,3]. In this regime, nonuniqueness of the wave angle  $\beta$  leads to the possibility of a “weak” or a “strong” shock.

TABLE I. Phase transitions in superfluid flow past a corner. The shapes correspond to Fig. 2 (inset) and Figs. 3(a)–3(d).

	Supersonic ( $M_2 > 1$ )	Subsonic ( $M_2 < 1$ )
$\theta < \beta$	Convective DSW $\diamond$	Detached DSW $\square$
$\theta > \beta$	Convective and turbulent $\circ$	Detached and turbulent $\triangle$

The oblique DSW jump conditions can be used to approximate flows past an obstacle. To study these dynamics we perform numerical simulations of Eq. (1) with  $\varepsilon=0.025$ , an initially quiescent fluid, and a repulsive (positive) potential  $V(x, y, t)$  that models a corner impulsively accelerated at  $t=0$  to a constant velocity. This “corner” is manifested by a rapid transition from  $V=0$  to a suitable large value at the corner’s boundary. Wherever the potential is large, there is negligible density so the potential acts as an effective boundary for the flow. The condition on the fluid flow at the boundary is then  $\vec{u} \cdot \hat{n}_\theta = 0$ . We assume the existence of an oblique DSW satisfying Eq. (7) and compare the predicted downstream flow conditions with the numerical simulations. Figure 3 shows example computational results.

Each subplot in Fig. 3 corresponds to a different choice of  $M_1$  and corner angle  $\theta$ , which are depicted by the geometric shapes in Fig. 2 and inset. Figure 3(a) shows a quasistationary oblique DSW emanating from the corner that satisfies the flow boundary conditions. Vortex pairs form far from the corner which is indicative of a convective instability [13]. Figure 3(b) shows a detached, curved DSW with vortices and waves propagating away from the corner. Figure 3(c) shows turbulent behavior that is convected away from the corner. Finally, Fig. 3(d) shows the most “violent” dynamics, which resemble fully developed turbulence in a viscous flow. Whereas the formation of vortices from dark stripes in these systems is well known [26], the varying behaviors depicted in Figs. 3(a)–3(d) are a consequence of the oblique DSW jump conditions in Eqs. (7) and (9).

We have performed many simulations while varying  $M_1$  and  $\theta$ . We now summarize the resulting dynamics referring to the shapes in Fig. 2, inset, and Fig. 3—see also Table I. ( $\diamond$ ) When the downstream flow is supersonic and the corner angle is smaller than the wave angle, the DSW experiences a convective instability and remains regular near the corner. ( $\square$ ) When the downstream flow is subsonic, the DSW becomes curved and detached from the corner accompanied by waves propagating ahead of the corner. An absolute transverse instability leads to the proliferation of vortices. ( $\circ$ ) When the corner angle is greater than the flow angle (the *cavitation regime*) a pure oblique DSW cannot exist. These “inadmissible” angles are manifested by the onset of turbulent dynamics which are convected away from the corner. ( $\triangle$ ) When the downstream flow is subsonic and the angles are inadmissible, the flow becomes both detached and turbulent.

We have verified the analytical results by extracting the downstream density  $\rho_2$  and Mach number  $M_2$  from the numerical simulations of flows past a corner in the convective DSW regime with  $M_1=2.3$  and find excellent agreement with

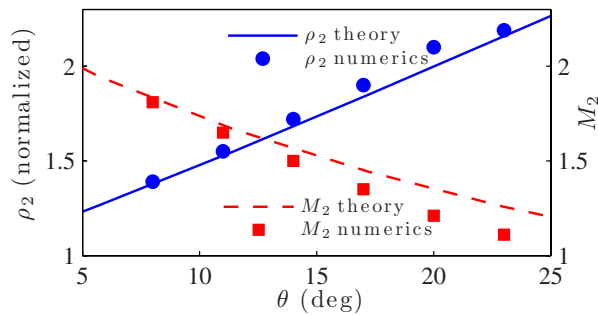


FIG. 4. (Color online) Predicted [Eqs. (6), (7), and (9)] and computed downstream density  $\rho_2$  (solid, circles) and Mach number  $M_2$  (dashes, squares) as a function of corner angle  $\theta$  with fixed  $M_1=2.3$  in the convective DSW regime  $\theta < \beta$ ,  $M_2 > 1$ .

the values predicted by Eqs. (6), (7), and (9) (see Fig. 4). Furthermore, the predicted wave angle  $\beta$  also agrees very

well with the numerical simulations [see dashed line in Fig. 3(a)].

In conclusion, we have obtained the jump conditions for 2D, oblique DSWs and used them to classify the behavior of supersonic flows past a corner. In contrast to viscous 2D flows, we find that 2D supersonic dispersive flows experience a range of phase transitions from stabilized convective flow patterns to violently unstable transonic flows leading to turbulence. These results demonstrate the use of oblique DSWs as building blocks for 2D supersonic flows and have potential application to the control of matter or optical waves and the generation of turbulence in condensed-matter physics and optics.

*Note added.* Recently, a publication appeared on stationary 2D NLS flows in the hypersonic ( $M_1 \gg 1$ ), small corner angle ( $0 < \theta \ll 1$ ) limit [27].

M.A.H. acknowledges support from the National Science Foundation under Grant No. DMS-0803074.

- [1] H. W. Liepmann and A. Roshko, *Elements of Gasdynamics* (Wiley, New York, 1957).
- [2] M. V. Dyke, *An Album of Fluid Motion* (Parabolic Press, Stanford, CA, 1982).
- [3] X. Cui, J. M. N. T. Gray, and T. Jhannesson, *J. Geophys. Res.* **112**, F04012 (2007).
- [4] N. F. Smyth and P. E. Holloway, *J. Phys. Oceanogr.* **18**, 947 (1988).
- [5] R. J. Taylor, D. R. Baker, and H. Ikezi, *Phys. Rev. Lett.* **24**, 206 (1970).
- [6] Z. Dutton, M. Budde, C. Slowe, and L. V. Hau, *Science* **293**, 663 (2001); T. P. Simula *et al.*, *Phys. Rev. Lett.* **94**, 080404 (2005).
- [7] M. A. Hofer *et al.*, *Phys. Rev. A* **74**, 023623 (2006).
- [8] J. E. Rothenberg and D. Grischkowsky, *Phys. Rev. Lett.* **62**, 531 (1989); W. Wan, S. Jia, and J. W. Fleischer, *Nat. Phys.* **3**, 46 (2007); C. Conti, A. Fratallocchi, M. Peccianti, G. Ruocco, and S. Trillo, *Phys. Rev. Lett.* **102**, 083902 (2009).
- [9] A. V. Gurevich, A. L. Krylov, V. V. Khodorovskii, *Sov. Phys. JETP* **82**, 709 (1996); **81**, 87 (1995).
- [10] G. El and A. Kamchatnov, *Phys. Lett. A* **350**, 192 (2006).
- [11] G. A. El, A. Gammal, and A. M. Kamchatnov, *Phys. Rev. Lett.* **97**, 180405 (2006).
- [12] Y. G. Gladush, G. A. El, A. Gammal, and A. M. Kamchatnov, *Phys. Rev. A* **75**, 033619 (2007).
- [13] A. M. Kamchatnov and L. P. Pitaevskii, *Phys. Rev. Lett.* **100**, 160402 (2008).
- [14] I. M. Krichever, *Funct. Anal. Appl.* **22**, 200 (1989).
- [15] M. A. Hofer, M. J. Ablowitz, and P. Engels, *Phys. Rev. Lett.* **100**, 084504 (2008).
- [16] I. Carusotto, S. X. Hu, L. A. Collins, and A. Smerzi, *Phys. Rev. Lett.* **97**, 260403 (2006); J. J. Chang, P. Engels, and M. A. Hofer, *ibid.* **101**, 170404 (2008).
- [17] C. N. Weiler *et al.*, *Nature (London)* **455**, 948 (2008).
- [18] E. A. L. Henn, J. A. Seman, G. Roati, K. M. F. Magalhães, and V. S. Bagnato, *Phys. Rev. Lett.* **103**, 045301 (2009).
- [19] C. J. Pethick and H. Smith, *Bose-Einstein Condensation in Dilute Gases* (Cambridge University Press, Cambridge, England, 2001).
- [20] R. W. Boyd, *Nonlinear Optics* (Academic Press, New York, 1991).
- [21] R. Y. Chiao, *Opt. Commun.* **179**, 157 (2000).
- [22] A. V. Gurevich and A. L. Krylov, *Sov. Phys. JETP* **65**, 944 (1987).
- [23] G. A. El, V. V. Geogjaev, A. V. Gurevich, and A. L. Krylov, *Physica D* **87**, 186 (1995).
- [24] See [7,23] for a discussion of vacuum points in 1D.
- [25] See EPAPS Document No. E-PLRAAN-80-R13911 for animations and momentum plot. For more information on EPAPS, see <http://www.aip.org/pubservs/epaps.html>
- [26] A. V. Mamaev, M. Saffman, and A. A. Zozulya, *Phys. Rev. Lett.* **76**, 2262 (1996).
- [27] G. A. El, A. M. Kamchatnov, V. V. Khodorovskii, E. S. Annibale, and A. Gammal, *Phys. Rev. E* **80**, 046317 (2009).